

Figure S1. Schematic diagram of semicontinuous reactor utilized for photocatalytic degradation tests: 1) AR14 solution, (2) magnetic stirrer, (3) control valve, (4) peristaltic pump, (6) reactor, (7) IR and UV filters, (8) Xenon lamp, (9) Xenon lamp power supply, (10) cooling fan and (11) sampling valve.

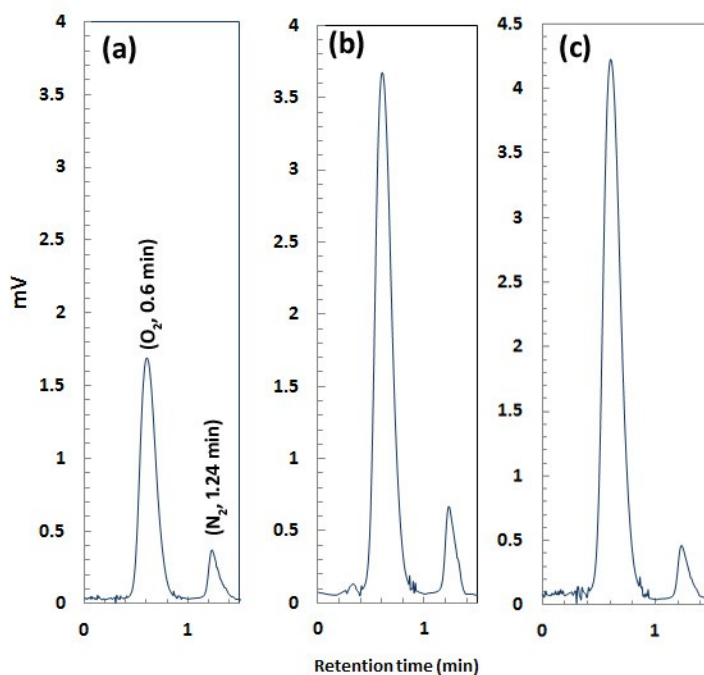


Figure S2. Typical GC traces of the head space in the photocatalytic oxygen evolution in the presence of (a) MnZnAl-LDH, (b) Co/ZnS and (c) Mn/ZnS samples (photocatalyst dosage=15 mg and Ag⁺ concentration=0.01 M). The evolved oxygen gas was analyzed by gas chromatography equipped with thermal conductivity detector (TCD) and a packed GC column with 5Å molecular sieves (Agilent, GC-7890A) with an argon carrier. During the water splitting reaction under solar simulated irradiation the reactor was kept under Argon flow. After desired irradiation time, the Xenon lamp was turned off and the reaction cell was shaken to equilibrate O₂ concentrations in liquid and gas phases. Then, 0.1 mL of the headspace gas was sampled by a deaired gastight syringe and analyzed for oxygen evolved during photocatalytic water splitting. To eliminate the oxygen content originated from contamination of the headspace of reactor by air, the nitrogen gas in the reactor headspace was quantified. From the nitrogen content, the oxygen content related to the air in headspace was calculated and subsequently subtracted from the total O₂ content to determine the amount of the O₂ produced during photocatalytic water splitting. When 0-1% air in Ar samples were injected into GC, the ratio of O₂ and N₂ peak areas was about 0.45.

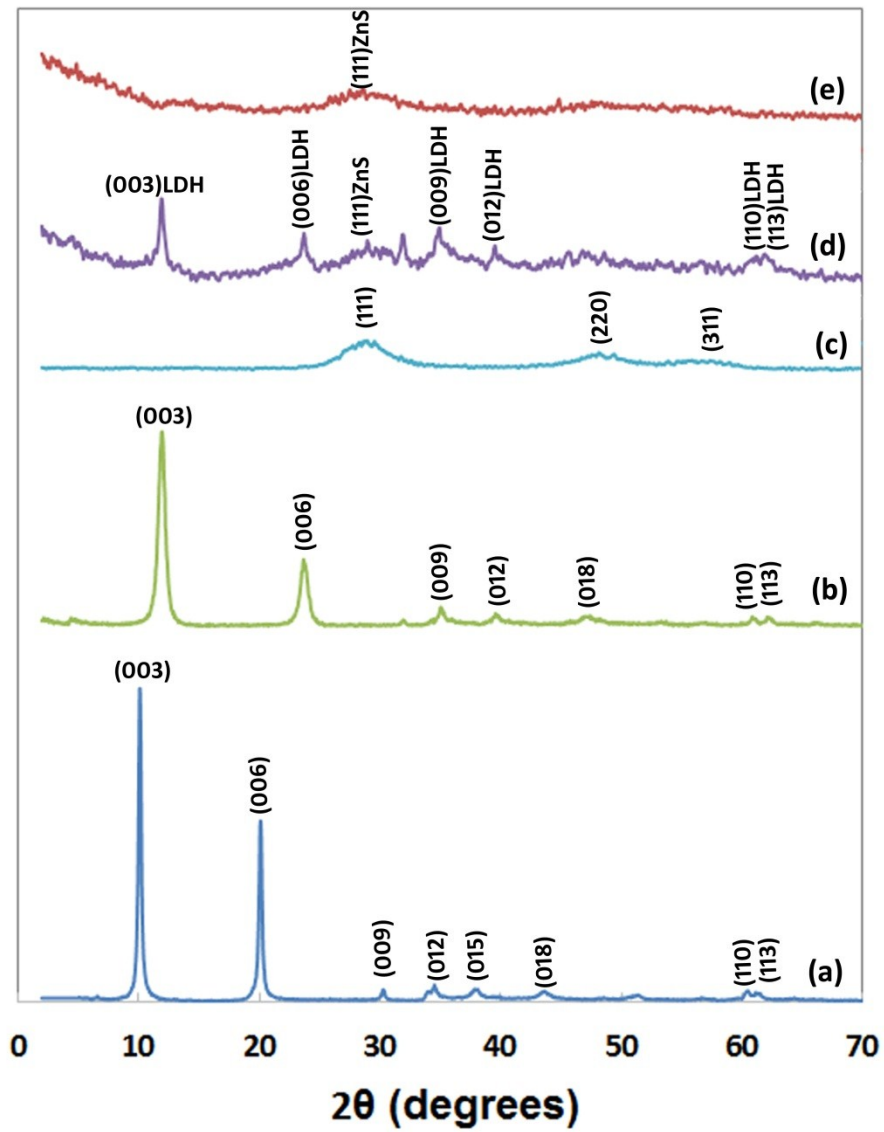


Figure S3. XRD pattern of (a) ZnAl-LDH, (b) NiZnAl-LDH, (c) ZnS QDs, (d) NiZnAl-LDH/QD, (e) NiZnAl-LDH/QD sample.

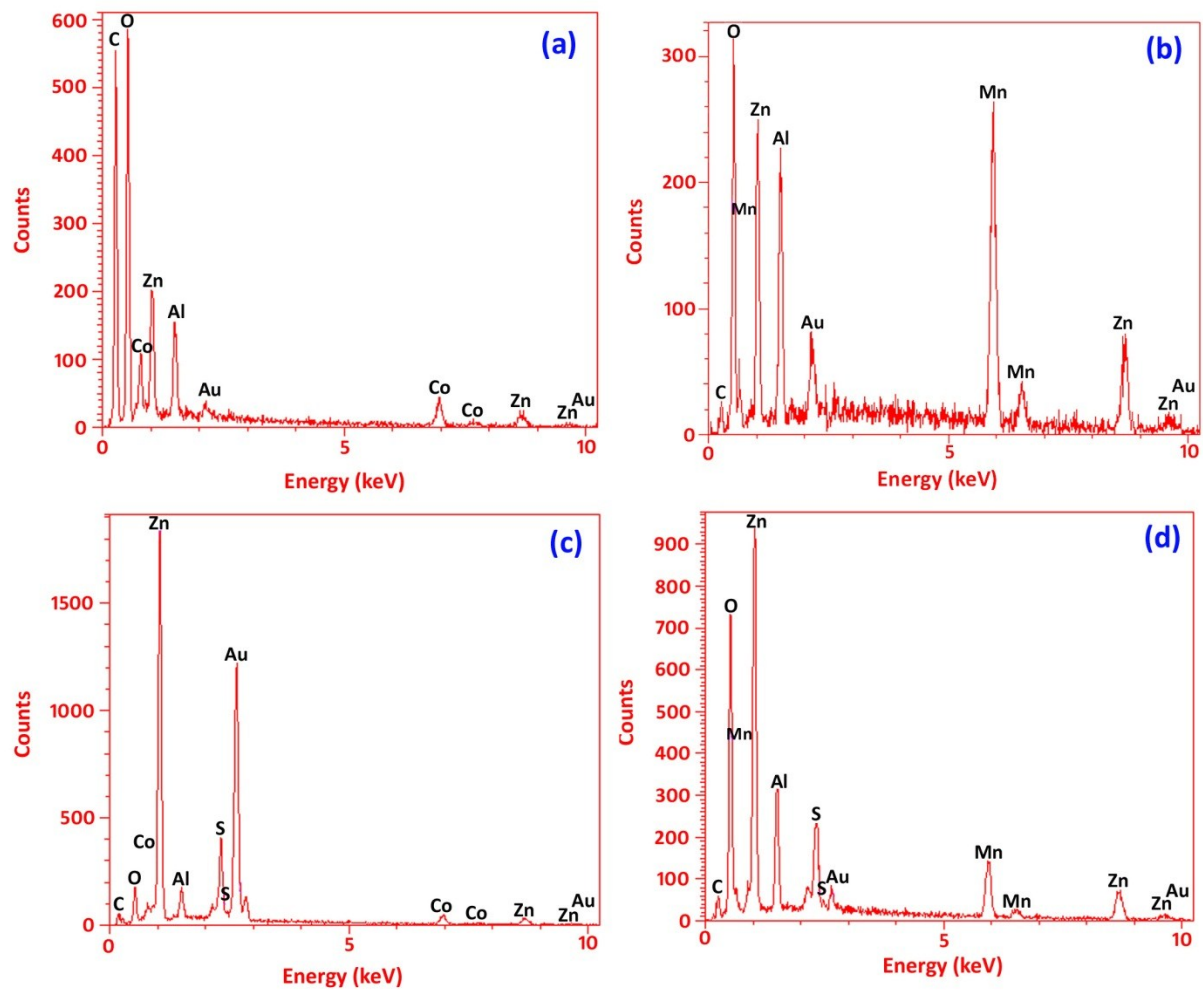


Figure S4. EDX pattern of (a) CoZnAl-LDH, (b) MnZnAl-LDH, (c) CoZnAl-LDH/QD and (d) MnZnAl-LDH/QD samples.

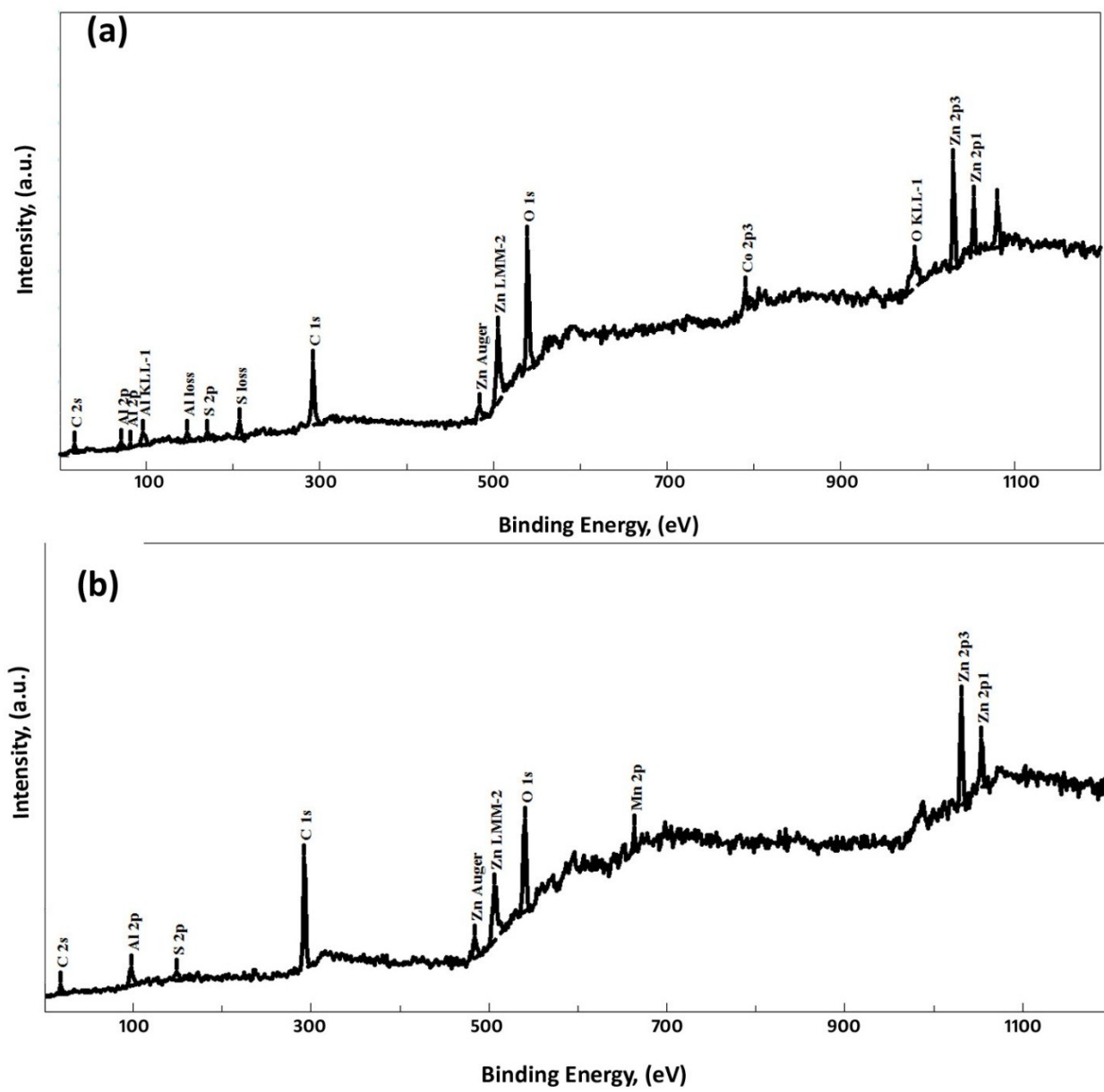


Figure S5. XPS spectra for (a) CoZnAl-LDH/QD and (b) MnZnAl-LDH/QD samples.

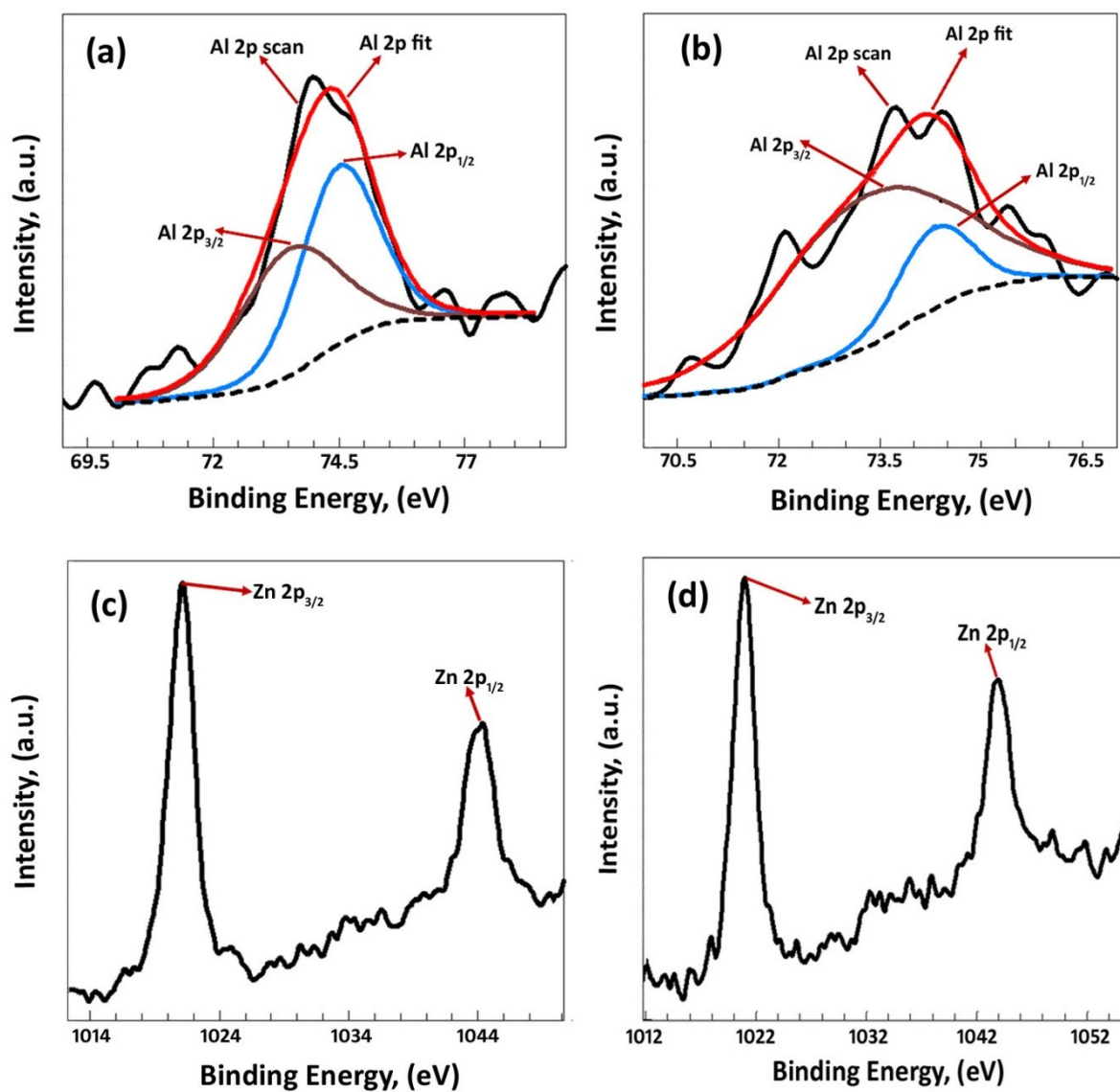


Figure S6. XPS high resolution spectra of (a) Al 2p for CoZnAl-LDH/QD, (b) Al 2p for MnZnAl-LDH/QD, (c) Zn 2p for CoZnAl-LDH/QD and (d) Zn 2p for MnZnAl-LDH/QD.

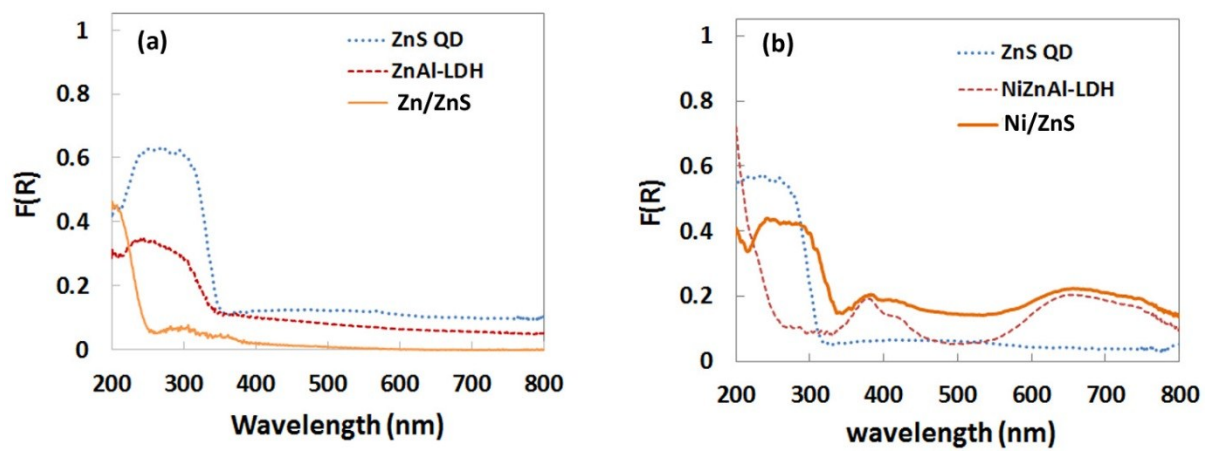


Figure S7. DRS spectra of (a) ZnAl-LDH and Zn/ZnS samples, and (b) NiZnAl-LDH and Ni/ZnS samples.

Table S1. QDs/binary M^{II}M^{III}-LDH hetrostructures and their different applications

LDH/QD	Synthesis Method	Intercalation of QDs in the LDH*	Application	Ref.
ZnCr /CdS	Self-assembly	No	Visible-Light-Induced H ₂ Generation	1
ZnCr /CdSe	Self-assembly	No	Visible-Light-Induced H ₂ Generation	2
ZnCr /CdS	Self-assembly	Yes	Visible-Light-Induced H ₂ Generation	3
NiFe/CdTe-CdS	Colloidal deposition	No	Visible-Light-Induced H ₂ Generation	4
CdAl/CdS	Gas/Solid Reaction	No	Photocatalytic degradation of Rhodamine B under visible light irradiation	5
MgAl/CdTe	Layer by Layer	No	Multicolor light emission	6
MgAl/CdTe	Layer by Layer	No	LEDs	7
MgAl/CdSe	Self-assembly	Yes	Optical behavior was studied	8
NiFe/Carbon	In situ growth	No	Electrocatalyst for water oxidation	9
MgAl/Carbon	Colloidal deposition	No	Adsorption of an organic dye (Methyl Blue)	10
MgAl/CdTe		No	Nitrite sensing (by chemiluminescence)	11
MgAl/CdTe	Immobilization of QDs on the surface of LDH by Self-assembly	No	Novel chemiluminescence probe	12
ZnAl/InP-ZnS core shell	In situ growth	Yes	Photoluminescence, quantum yields and thermal- and photostability were enhanced.	13
ZnAl/Carbon	In situ growth	No	Adsorption of Cd ²⁺ from contaminated water	14
CoFe/Carbon	Colloidal deposition	No	Hydrogen peroxide sensing	15
CoAl/CdTe	Layer by Layer	No	Trinitrotoluene sensor	16
NiAl/Carbon	In situ growth	No	Supercapacitors	17

* Is the evidence exhibited for intercalation of QDs in the interlayer space of the LDHs?

Table S2. LDH based photocatalysts and their efficiencies in photocatalytic O₂ evolution and degradation of the organic pollutants.

Photocatalyst	Target	Experimental conditions	Activity	Ref.
NiTi-LDH	MB ^a	300 W Xenon lamp ($\lambda \geq 420$ nm), 0.4 mg/L of dye and 100 mg/L of Cat.	99% (75 min)	18
g-C ₃ N ₄ /NiFe-LDH	H ₂ O	125 W medium pressure Hg lamp ($\lambda \geq 420$ nm)	443 $\mu\text{mol/g.h O}_2$, (163.5 $\mu\text{mol/g.h O}_2$ for pristine LDH)	19
ZnFe-LDH	MV ^b MG ^c	Sun illumination (104000 Lx), 100 mg/L of dye and 1 g/L of Cat.	$\geq 98\%$ (120 min)	20
Terbium doped ZnCr-LDH	H ₂ O	150 W Xenon lamp, ($\lambda \geq 420$ nm)	1022 $\mu\text{mol/g.h O}_2$, (543 $\mu\text{mol/g.h O}_2$ for pristine LDH)	21
CdS/CoAl-LDH	AR88 ^d	500 W Xenon lamp ($\lambda \geq 420$ nm), 100 mg/L of MB and 300 mg/L of Cat.	90% (180 min), (55% for pristine LDH)	22
ZnTi-LDH	MB	300 W Xenon lamp, ($\lambda \geq 420$ nm), 5 mg/L of dye and 1 g/L of Cat.	100% (100 min)	23
MnCr-LDH	MB	Visible illumination ($360 \leq \lambda \leq 800$ nm), 30 mg/L of dye and 5 mg/L of Cat.	90% (300 min)	24
MgZnAl-CLDH	Phenol	UV illumination 254 nm, 300 mg/L of Pollutant and 1 g/L of Cat.	97% (540 min)	25
CoFe-LDH	H ₂ O	300 W Xenon lamp ($\lambda \geq 420$ nm)	333 $\mu\text{mol/g.h O}_2$	26
Zn/M-LDHs (M = Al, Fe, Ti)	RhB ^e	150W halogen lamp ($380 \leq \lambda \leq 760$ nm), 3 mg/L of dye and 666 mg/L of Cat.	98% for ZnTi-LDH (120 min) 96% for ZnAl-LDH (120 min) 72% for ZnFe-LDH (120 min)	27
ZnTiFe-LDH	RhB	150W halogen lamp ($380 \leq \lambda \leq 760$ nm), 3 mg/L of dye and 666 mg/L of Cat.	88% (120 min)	27
ZnTi, ZnCe and ZnCr LDH	H ₂ O	200 W xenon-doped mercury lamp ($\lambda \geq 420$ nm)	1022 $\mu\text{mol/g.h O}_2$ (for ZnCr) 268.3 $\mu\text{mol/g.h O}_2$ (for ZnTi) 626.1 $\mu\text{mol/g.h O}_2$ (for ZnCe) 90% for CoCr-LDH	28
M ^{II} /Cr-LDHs (M=Co, Ni, Cu, and Zn)	MO ^f	Visible illumination ($360 \leq \lambda \leq 800$ nm), 100 mg/L of dye and 1 g/L of Cat.	(180 min) 68% for NiCr-LDH 75% for CuCr-LDH 80% for ZnCr-LDH	29
NiZnAl-LDHs	OG ^g	Sun illumination (74000 Lx), 50 mg/L of dye and 500 mg/L of Cat.	99% (100 min)	30
MnCoTi-LDHs	RhB	Tungsten lamp ($\lambda \geq 400$ nm), 4.79 mg/L of dye and 75 mg/L of Cat.	99% (60 min)	31

a: Methylene Blue, b: Methyl Violet, c: Malachite Green, d: Acid Red 88, e: Rhodamin B, f: Methyl Orange, g: Orange G

Table S3. LDH based heterostructures used in various photocatalytic applications.

Photocatalyst	Target	Experimental conditions	Activity	Ref.
Cs _{0.33} WO ₃ /CoAl-LDH	Tetracycline	500 W Xenon lamp ($\lambda \geq 420$ nm), 40 mg/L of Pollutant and 1 g/L of Cat.	91.2% (270 min)	32
Cu ₂ O/MgAl-LDH	Orange II	120 W LED ($\lambda \geq 420$ nm), 40 mg/L of Pollutant and 1 g/L of Cat.	90% (300 min)	33
g-C ₃ N ₄ /ZnIn-CLDH	RhB	300 W Xenon lamp ($\lambda \geq 420$ nm), 10 mg/L of Pollutant and 1 g/L of Cat.	100% (60 min)	34
TiO ₂ /CuMgAl-LDH	MB	300 W Xenon lamp ($\lambda \geq 420$ nm), 3.2 mg/L of Pollutant and 300 mg/L of Cat.	67% (400 min)	35
ZnS/ZnAl-LDH	RhB	UV illumination 254 nm, 4 mg/L of Pollutant and 1 g/L of Cat.	94% (180 min)	36
Graphene/ZnCr-LDH	RhB	300 W Xenon lamp ($\lambda \geq 420$ nm), 10 mg/L of Pollutant and 1 g/L of Cat.	92% (140 min)	34
g-C ₃ N ₄ /NiAl-LDH	RhB	500 W high-pressure Hg lamp, 10 mg/L of Pollutant and 600 mg/L of Cat.	$\geq 90\%$ for MO (180 min) $\geq 99\%$ for RhB (240 min)	37
RGO/NiTi-LDH	H ₂ O	300 W Xenon lamp ($\lambda \geq 420$ nm)	1968 $\mu\text{mol/g.h O}_2$	38
CdS/CdAl-LDH	RhB	500 W high-pressure Hg lamp, 50 mg/L of Pollutant and 1g/L of Cat.	$\geq 90\%$ (120 min)	5
Layered titanium oxide/ZnCr-LDH	H ₂ O	500 W xenon lamp ($\lambda \geq 420$ nm)	1180 $\mu\text{mol/g.h O}_2$	39

Table S4. ZnS QDs based photocatalysts and their photocatalytic applications.

Photocatalyst	Target	Experimental conditions	Activity	Ref.
Cu-doped ZnS QDs/TiO ₂	Salicylic acide	Fluorescent lamp (365 nm, I = 1.5 mW/cm ²), 10 mg/L of Pollutant.	90% (150 min)	40
ZnS QDs/chitosan	MB MO	Ultraviolet-C (UVC= 280–100 nm), 20 mg/L of Pollutant and 30 mg/L of Cat.	90% for MB (120 min) 68% for MO (240 min)	41
ZnS QDs/RGO	MB	High pressure Hg lamp (365 nm), 10 mg/L of Pollutant and 200 mg/L of Cat.	≥90% (120 min)	42
ZnS QDs-MgAl	MB	High pressure Hg lamp (365 nm), 10 mg/L of Pollutant and 20 mg/L of Cat.	95% (150 min)	43
ZnS QDs-TiO ₂ nanofibers	MB	UV lamp (365 nm), 10 mg/L of Pollutant and photocatalyst films (area of 1×1 cm ² .	≥90% (450 min)	44
Mn-doped ZnS QDs	MO	8 W mercury vapour lamp (365 nm), 10 mg/L of Pollutant and 1 g/L of Cat.	94.5% (120 min)	45
Tb-doped ZnS QDs	CV	4W UV lamp (254 nm), 500 mg/L of Cat.	85% (120 min)	46
Fe-doped ZnS QDs	MG	40W UV lamp, 10 mg/L of Pollutant and 90 mg/L of Cat.	90% (90 min)	47
ZnS QDs-mesoporus TiO ₂	MB	Xenon lamp, 10 mg/L of Pollutant and 50 mg/L of Cat.	100% (32 min)	48
M-doped ZnS QDs (M=Cu, Mn &Ag)	VB ^a	40W UV lamp, 10 mg/L of Pollutant and 90 mg/L of Cat.	100% (90 min)	49
CuInS ₂ /ZnS QDs	H ₂ O (Hydrogen evolution)	150 W Xenon lamp ($\lambda \geq 420$ nm)	1590 μ mol/g.h H ₂	50
Ga-doped ZnS QDs	Phenol red	UV illumination	≥95% (140 min)	51
CuInS ₂ /ZnS QDs	RhB	500 W high-pressure Hg lamp ($\lambda \geq 420$ nm), 10 mg/L of Pollutant and 600 g/L of Cat.	≥95% (120 min)	52
ZnS QDs/MZnAl-	AR14	300 W Xenon lamp ($\lambda \geq 420$	≥95% (60 min)	This

LDH (M=Co or Mn)		nm), 50 mg/L of Pollutant and 200 mg/L of Cat.		Work
ZnS QDs/MZnAl-LDH (M=Co or Mn)	H ₂ O	300 W Xenon lamp ($\lambda \geq 420$ nm), 50 mg/L of Pollutant and 200 mg/L of Cat.	For M=Co, 1056 $\mu\text{mol/g. h O}_2$ For M=Mn, 1246 $\mu\text{mol/g. h O}_2$	This Work

a: Victoria Blue

- J. M. Lee, J. L. Gunjekar, Y. Ham, I. Y. Kim, K. Domen and S.-J. Hwang, *Chemistry – A European Journal*, 2014, **20**, 17004 – 17010.
- G. Zhang, B. Lin, Y. Qiu, L. He, Y. Chen and B. Gao, *International Journal of Hydrogen Energy*, 2015, **40**, 4758-4765.
- G. Zhang, B. Lin, W. Yang, S. Jiang, Q. Yao, Y. Chen and B. Gao, *RSC Advances*, 2015, **5**, 5823-5829.
- D. Yue, X. Qian, M. Kan, M. Ren, Y. Zhu, L. Jiang and Y. Zhao, *Applied Catalysis B: Environmental*, 2017, **209**, 155-160.
- Y. Guo, H. Zhang, Y. Wang, Z.-L. Liao, G.-D. Li and J.-S. Chen, *The Journal of Physical Chemistry B*, 2005, **109**, 21602-21607.
- R. Liang, S. Xu, D. Yan, W. Shi, R. Tian, H. Yan, M. Wei, D. G. Evans and X. Duan, *Advanced Functional Materials*, 2012, **22**, 4940-4948.
- J. S. Bendall, M. Paderi, F. Ghigliotti, N. Li Pira, V. Lambertini, V. Lesnyak, N. Gaponik, G. Visimberga, A. Eychmüller, C. M. S. Torres, M. E. Welland, C. Gieck and L. Marchese, *Advanced Functional Materials*, 2010, **20**, 3298-3302.
- B. R. Venugopal, N. Ravishankar, C. R. Perrey, C. Shivakumara and M. Rajamathi, *The Journal of Physical Chemistry B*, 2006, **110**, 772-776.
- D. Tang, J. Liu, X. Wu, R. Liu, X. Han, Y. Han, H. Huang, Y. Liu and Z. Kang, *ACS applied materials & interfaces*, 2014, **6**, 7918-7925.
- M. Zhang, Q. Yao, C. Lu, Z. Li and W. Wang, *ACS applied materials & interfaces*, 2014, **6**, 20225-20233.
- S. Dong, W. Guan and C. Lu, *Sensors and Actuators B: Chemical*, 2013, **188**, 597-602.
- S. Dong, F. Liu and C. Lu, *Analytical chemistry*, 2013, **85**, 3363-3368.
- S. Cho, S. Jung, S. Jeong, J. Bang, J. Park, Y. Park and S. Kim, *Langmuir*, 2012, **29**, 441-447.
- O. Rahmanian, M. Dinari and M. K. Abdolmaleki, *Applied Surface Science*, 2018, **428**, 272-279.
- Y. Wang, Z. Wang, Y. Rui and M. Li, *Biosensors and Bioelectronics*, 2015, **64**, 57-62.
- Z. Li, Y. Zhou, D. Yan and M. Wei, *Journal of Materials Chemistry C*, 2017, **5**, 3473-3479.
- Y. Wei, X. Zhang, X. Wu, D. Tang, K. Cai and Q. Zhang, *RSC Advances*, 2016, **6**, 39317-39322.
- P. R. Chowdhury and K. G. Bhattacharyya, *Dalton Transactions*, 2015, **44**, 6809-6824.
- S. Nayak, L. Mohapatra and K. Parida, *Journal of Materials Chemistry A*, 2015, **3**, 18622-18635.
- K. Parida and L. Mohapatra, *Chemical engineering journal*, 2012, **179**, 131-139.
- Y. Fu, F. Ning, S. Xu, H. An, M. Shao and M. Wei, *Journal of Materials Chemistry A*, 2016, **4**, 3907-3913.
- Y. Qiu, B. Lin, F. Jia, Y. Chen, B. Gao and P. Liu, *Materials Research Bulletin*, 2015, **72**, 235-240.
- M. Shao, J. Han, M. Wei, D. G. Evans and X. Duan, *Chemical engineering journal*, 2011, **168**, 519-524.
- Z. Timár, G. Varga, S. Muráth, Z. Kónya, Á. Kukovecz, V. Havasi, A. Oszkó, I. Pálincó and P. Sipos, *Catalysis Today*, 2017, **284**, 195-201.
- J. S. Valente, F. Tzompantzi, J. Prince, J. G. H. Cortez and R. Gomez, *Applied Catalysis B: Environmental*, 2009, **90**, 330-338.
- S. J. Kim, Y. Lee, D. K. Lee, J. W. Lee and J. K. Kang, *Journal of Materials Chemistry A*, 2014, **2**, 4136-4139.
- S.-J. Xia, F.-X. Liu, Z.-M. Ni, J.-L. Xue and P.-P. Qian, *Journal of Colloid and Interface Science*, 2013, **405**, 195-200.

28. C. G. Silva, Y. Bouizi, V. FornΓ©s and H. GarcιMΓa, *Journal of the American Chemical Society*, 2009, **131**, 13833-13839.
29. N. Baliarsingh, K. Parida and G. Pradhan, *Industrial & Engineering Chemistry Research*, 2014, **53**, 3834-3841.
30. X. Wang, P. Wu, Y. Lu, Z. Huang, N. Zhu, C. Lin and Z. Dang, *Separation and Purification Technology*, 2014, **132**, 195-205.
31. P. R. Chowdhury and K. G. Bhattacharyya, *RSC Advances*, 2016, **6**, 112016-112034.
32. D. Zhang, T. Ji, J. Yu, X. Jiang and F. Jiao, *Photochemistry and Photobiology*, 2018, **94**, 219-227.
33. J. Ma, J. Ding, L. Li, J. Zou, Y. Kong and S. Komarneni, *Ceramics International*, 2015, **41**, 3191-3196.
34. M. Lan, G. Fan, L. Yang and F. Li, *RSC Advances*, 2015, **5**, 5725-5734.
35. R. Lu, X. Xu, J. Chang, Y. Zhu, S. Xu and F. Zhang, *Applied Catalysis B: Environmental*, 2012, **111-112**, 389-396.
36. Z. Li, M. Chen, Q. Zhang, J. Qu, Z. Ai and Y. Li, *Applied Clay Science*, 2017, **144**, 115-120.
37. G. Salehi, R. Abazari and A. R. Mahjoub, *Inorganic Chemistry*, 2018, **57**, 8681-8691.
38. B. Li, Y. Zhao, S. Zhang, W. Gao and M. Wei, *ACS applied materials & interfaces*, 2013, **5**, 10233-10239.
39. J. L. Gunjekar, T. W. Kim, H. N. Kim, I. Y. Kim and S.-J. Hwang, *Journal of the American Chemical Society*, 2011, **133**, 14998-15007.
40. H. Labiadh, T. B. Chaabane, L. Balan, N. Becheik, S. Corbel, G. Medjahdi and R. Schneider, *Applied Catalysis B: Environmental*, 2014, **144**, 29-35.
41. A. A. P. Mansur, H. S. Mansur, F. P. Ramanery, L. C. Oliveira and P. P. Souza, *Applied Catalysis B: Environmental*, 2014, **158-159**, 269-279.
42. M. Wei, Y. Hong, D. Han, L. Yang, H. Liu and L. Su, *physica status solidi (a)*, 2018, **215**, 1800082.
43. K. Bhuvaneshwari, G. Palanisamy, T. Pazhanivel, G. Bharathi and D. Nataraj, *ChemistrySelect*, 2018, **3**, 13419-13426.
44. S. Chaguetmi, F. Mammeri, S. Nowak, P. Decorse, H. Lecoq, M. Gaceur, J. Ben Naceur, S. Achour, R. Chtourou and S. Ammar, *RSC Advances*, 2013, **3**, 2572-2580.
45. S. Joicy, R. Saravanan, D. Prabhu, N. Ponpandian and P. Thangadurai, *RSC Advances*, 2014, **4**, 44592-44599.
46. B. Poornaprakash, U. Chalapathi, Y. Suh, S. V. P. Vattikuti, M. S. P. Reddy and S.-H. Park, *Ceramics International*, 2018, **44**, 11724-11729.
47. H. R. Rajabi, O. Khani, M. Shamsipur and V. Vatanpour, *Journal of Hazardous Materials*, 2013, **250-251**, 370-378.
48. S. Harish, M. Sabarinathan, A. P. Kristy, J. Archana, M. Navaneethan, H. Ikeda and Y. Hayakawa, *RSC Advances*, 2017, **7**, 26446-26457.
49. H. R. Rajabi, F. Karimi, H. Kazemdehdashti and L. Kavoshi, *Journal of Photochemistry and Photobiology B: Biology*, 2018, **181**, 98-105.
50. M. Sandroni, R. Gueret, K. D. Wegner, P. Reiss, J. Fortage, D. Aldakov and M. N. Collomb, *Energy & Environmental Science*, 2018, **11**, 1752-1761.
51. B. Poornaprakash, U. Chalapathi, S. V. P. Vattikuti, M. C. Sekhar, B. P. Reddy, P. T. Poojitha, M. S. P. Reddy, Y. Suh and S.-H. Park, *Ceramics International*, 2019, **45**, 2289-2294.
52. W. Zhang and X. Zhong, *Inorganic Chemistry*, 2011, **50**, 4065-4072.